## Title
Focal ablation of prostate cancer: four roles for magnetic resonance imaging guidance.



## Journal
Canadian journal of urology, 20(2)

## ISSN
1195-9479

## Authors
Sommer, Graham
Bouley, Donna
Gill, Harcharan
et al.

## Publication Date
2013-04-01

Peer reviewed

Published in final edited form as:
*Can J Urol*. 2013 April ; 20(2): 6672–6681.

# Focal Ablation of Prostate Cancer: Four Roles for MRI Guidance

**Graham Sommer, MD**[1], **Donna Bouley, PhD,DVM**[2], **Harcharan Gill, MD**[3], **Bruce Daniel, MD**[1], **Kim Butts Pauly, PhD**[1], and **Christopher Diederich, PhD**[4]

[1]Department of Radiology, Standford University School of Medicine

[2]Department of Comparative Medicine, Standford University School of Medicine

[3]Department of Urology, Stanford University School of Medicine

[4]UCSF Department of Radiation Oncology

## Abstract

**Introduction—**There is currently a great deal of interest in the possible use of focal therapies for prostate cancer, since such treatments offer the prospect for control or cure of the primary disease with minimal side effects. Many forms of thermal therapy have been proposed for focal ablation of prostate cancer, including laser, high intensity ultrasound and cryotherapy. This review will demonstrate the important roles that MRI guidance can offer to such focal ablation, focusing on the use of high intensity ultrasonic applicators as an example of one promising technique.

**Materials and Methods—**Transurethral and interstitial high intensity ultrasonic applicators, designed specifically for ablation of prostate tissue were tested extensively in vivo in a canine model. The roles of MRI in positioning the devices, monitoring prostate ablation, and depicting ablated tissue were assessed using appropriate MRI sequences.

**Results—**MRI guidance provides a very effective tool for the positioning of ablative devices in the prostate, and thermal monitoring successfully predicted ablation of prostate tissue when a threshold of 52°C was achieved. Contrast enhanced MRI accurately depicted the distribution of ablated prostate tissue, which is resorbed at 30 days.

**Conclusions—**Guidance of thermal therapies for focal ablation of prostate cancer will likely prove critically dependent on MRI functioning in four separate roles. Our studies indicate that in 3 roles: device positioning; thermal monitoring of prostate ablation; and depiction of ablated prostate tissue, MR techniques are highly accurate and likely to be of great benefit in focal prostate cancer ablation. A fourth critical role, identification of cancer within the gland for targeting of thermal therapy, is more problematic at present, but will likely become practical with further technological advances.

### Keywords

Prostate Cancer; MRI; ablation; therapeutic ultrasound; focal treatment

Corresponding Author: Graham Sommer MD, Department of Radiology, room H1307 Stanford University Medical Center, 300 Pasteur Drive, Stanford CA 94305 Phone: 650-723-8463 Fax: 650-723-1909 gsommer@stanford.edu.

Conflict of Interest:
All authors declare that there are no competing financial interests in relation to the work described.

## Introduction

There has been substantial experience with techniques exploiting thermal effects for clinical ablation of prostate cancer, based on treatment of the entire prostate gland. Such studies have used such techniques such as high intensity focused ultrasound (HIFU)[1] and cryotherapy[2]. Limited clinical studies have demonstrated that such minimally invasive thermal approaches offer the possibility of effective focal, rather than whole gland, ablation of prostate tissue with minimal side effects compared to established procedures such as radical prostatectomy[3,4]. Recent analyses of such minimally invasive thermal approaches have indicated the desirability, and perhaps the necessity for accurate imaging guidance of such focally ablative techniques[5], with magnetic resonance imaging (MRI) the likely most effective imaging modality. MRI guidance in fact has the potential for assisting focally ablative procedures in a number of critical ways: by depicting cancer within the prostate gland to allow targeting of the cancer “index lesion”, aiding the positioning of applicators within or near the gland, monitoring treatment with magnetic resonance thermal imaging (MRTI) and displaying the distribution of prostate tissue ablation post-procedure. In this review, we will discuss the likelihood that prostate cancer can be treated effectively by ablating only those portions of the prostate gland actually containing cancer, and how this goal might be achieved using MRI-guidance. There is a wide range of potential forms of thermal therapy for focal prostatic ablation that might benefit from MRI guidance, including radiofrequency (RF)[1,3,6], laser[2,4,7], therapies in addition to HIFU and cryotherapy. The potential use of MRI-compatible transurethral and interstitial ultrasonic applicators will be presented as one promising approach to MRI-guided focal ablation of prostate cancer, and to illustrate several roles for MRI guidance.

## The potential utility of focal prostate cancer ablation

An important question is whether focal ablation of a major focus of prostate cancer within the gland will lead to effective treatment. It is well known that prostate cancer is a multifocal disease, and in the past this multifocal character has been suggested as a reason for complete removal or ablation of the prostate. In typical studies of prostate cancer mapping in radical prostatectomy specimens, for example[8-12], substantial majorities of specimens have multiple small foci of cancer, typically 2 or more, in addition to a larger focus of disease. A number of extensive pathologic studies of prostatectomy specimens, along with clinical correlation with the pathologic results, however, have given rise to the “index lesion” concept[5,13-16] of prostate cancer. In this view only the largest focus of cancer within the prostate, the index lesion, dominates the clinical picture, and ablation of this focus alone will provide effective treatment in a substantial majority of patients. In extensive pathological studies of prostatectomy specimens by McNeal and co workers[11,17,18], for example, it was noted that the likelihood of recurrent prostate cancer, and biochemical failure, was a function solely of the size and percentage of high Gleason grade tumor in the largest focus, or index lesion, of tumor. The likelihood of recurrence was not a function of the number or volume of smaller cancers, generally smaller in size than 0.5 cc. Additionally recent studies of the genomic analysis of prostate cancer metastasis have demonstrated the monoclonal nature of metastatic prostate cancer[19,20], providing further evidence that metastatic potential of

prostate cancer is related only to the presence of the largest or index lesion within the gland. These and other similar studies have provided strong support for the concept that ablation of the largest, generally highest grade tumor in the prostate, the index lesion, will provide effective treatment of confined prostate cancer.

## Roles of MRI: #1 Depiction of the prostate cancer “index lesion” within the gland

In the limited studies of clinical focal ablation to date, the need for accurate tumor localization has lead to the use of preprocedural localization techniques such as transperineal 3D mapping[10,21] (saturation biopsies), which may involve a median of 46 core biopsies obtained with the patient under general anesthesia or heavy i.v. sedation. Such time consuming and invasive techniques may not be practical for routine use, and MRI localization of tumor, if possible, would be much more attractive, rapid and noninvasive alternative. Accurate MRI depiction would allow the integration of MRI into the procedure as a tool with which to target the index lesion prior to the ablation procedure. While there have been a great many studies of the ability of MRI to depict prostate cancer within the gland, the accuracy of depiction can likely best be inferred from studies directly comparing preoperative MR imaging to step-section pathology of prostatectomy specimens interpreted on a blinded basis. The determination of effectiveness of MRI is made more complex by the fact that at least 4 variants of MR imaging have been evaluated for their abilities to localize focal prostate cancer in vivo, and the experimental designs and analyses in various studies have differed in important ways. Nonetheless, there have been several recent studies[22,23] at 1.5 Tesla employing the 4 standard MR techniques of interest, and using a standard technique of assessing the performance of an imaging test, ROC (Receiver Operator Characteristic) analysis, in depicting the largest tumor, or index lesion, within the prostate. In ROC analysis, plots of true positives against false positives are performed, often with several observers, and the AUC (Area Under the Curve) of the resulting plot is used to provide a measure of performance: using such an approach, an AUC of 1 would indicate perfect performance of a test, and an AUC of 0.5 would represent complete inability of a test to perform a task. AUC values in the range of 0.5 to 0.6 are generally interpreted as indicating a worthless test; values of 0.6 to 0.7 indicate poor performance, and 0.7 to 0.8 indicate fair performance.

Four MRI methods which have been extensively evaluated are standard T2-weighted imaging (T2W), magnetic resonance spectroscopic imaging (MRSI), diffusion-weighted imaging (DWI) and dynamic contrast enhanced (DCE) imaging. Early studies of T2W indicated that histologic correlation with such images was inaccurate due to a lack of specificity of MRI appearances for cancer[24,25]. In a more recent large multi-institutional study[23] at 1.5 T, ROC analysis was performed to evaluate the performance of T2W and MRSI in localization of the prostate cancer index lesion, and another recent study[22] evaluated T2W, DWI and DCE using a similar study design. The AUC values determined in the former study were 0.60 for T2W alone and 0.58 for MRSI interpreted along with the T2W; in the second smaller study, the AUC values for T2W, DCE and DWI respectively were 0.673, 0.592 (mapping the parameter $K_{trans}$ from the DCE), and 0.689. Overall, the

AUC values indicate rather poor performance for MRI in cancer localization, although the newer technique of DWI appears promising. In spite of these findings, it is likely that further improvements in the techniques for creating MR images, and higher field strength MR systems with greater SNR, will lead to better performance in the future. An example of imaging of prostate cancer in vivo with newer techniques, and at higher field strength, 3 Tesla, is shown in Figure 1. The scans are a recent preoperative MRI of a patient prior to radical prostatectomy, along with a diagram showing the location of the index cancer drawn from histopathologic analysis of the prostatectomy specimen. The images are from an ongoing HIPAA-compliant prospective study at our institution with IRB approval. The lesion appears to be identifiable using T2W (Figure 1A), and with advanced techniques of DWI with restricted field of view[26] (Figure 1B) and DCE[27] (Figure 1C), although the depiction of tumor in the various MR images does not conform perfectly to the pathologic mapping (Figure 1D). More recently developed DWI techniques using high values of the diffusion encoding parameter b[28,29] (Figure 1B, in which a high b value of acquisition was used (1600 s/mm$^2$)), have been shown particularly sensitive to the depiction of prostate cancer within the gland. In spite of its limitations, MRI has been proved more accurate than competing techniques such as ultrasound in depicting prostate cancer, and has been used successfully as a method for guiding biopsy for prostate cancer[30,31]. The suggestion has also been made that a “multiparametric” approach, in which the various forms of MRI are used in combination might be more effective than any single sequence, in localizing the index lesion within the prostate[22,32,33], and there are also indications from these and other studies[34] that larger tumors with more higher Gleason grade tumor are more readily detectable, and differ more in MRI characteristics, than smaller cancers. Since accurate targeting of cancer index lesions within the gland is required if focal ablative techniques are to be successful, the inconsistent ability of current MRI techniques to depict cancer accurately in the prostate appears likely to limit its utility as a localization tool in many cases. There is considerable promise, however, for improved accuracy of depiction, and perhaps even provision of some insight into tumor grading with MRI at higher field strengths, and using the most advanced techniques available.

## Role #2 for MRI: Positioning ablation devices within or near the prostate gland

Optimal positioning of thermally ablative devices within or adjacent to the prostate gland is another important role for MRI. Rapid T1 or T2 weighted images can be obtained in near real time as desired to guide and check positioning of such devices as lasers, cryotherapy probes, radiofrequency (RF) probes, and catheter-based ultrasonic devices prior to energy delivery and tissue ablation. Our group has developed ultrasound applicators[35-39] that can be positioned either transurethrally or directly into the prostatic parenchyma (interstitially) via a transperineal approach, and studies with such devices will be used below to illustrate the positioning, thermal monitoring, and postprocedural imaging involved in the ablative process. Such high power ultrasound emitting devices have important advantages in that they can be manufactured both so as to be MRI-compatible, and to deliver energy with precise directionality, whereas such techniques as laser heating and cryotherapy cooling are omnidirectional.

Schematic diagrams of the MRI-compatible transurethral and interstitial applicators, which have been tested for in vivo ablation of canine prostate, are represented in Figure 2. Three basic configurations for the piezoelectric emitter in the transurethral applicators (Figure 2A) have been evaluated: 90 to 120-degree sectored tubular, planar and lightly (weakly) focused active elements have been employed. Applicator configurations typically consisted of 2 or more transducer sections (3.5 mm. outer diameter or width, by 10 mm length, and 6.5 to 8 MHz operating frequency), mounted on a 4-6 mm delivery catheter with an inflatable 10-mm outer diameter cooling balloon, and a distal retention balloon. The transurethral devices can then be rotated while in place to target regions along a radial axis from the urethra. The applicators can be rotated along the urethral axis to ablate a number of desired regions in sequence if desired. Multiple appropriate rotation increments of any of these devices can be performed in order to target any desired angular sector in multiple heating steps.

MRI-compatible interstitial ultrasound applicators which may be inserted directly into the prostatic parenchyma have also been evaluated, as described by Nau et al.[40-44] in vivo. A schematic diagram of such an applicator is provided in Figure 2B. A typical device consists of an array of 2 or 3 cylindrical piezoelectric elements having outer diameter (OD) of 1.5 mm. and lengths of 10 mm. The outer surface of the transducers were sectored to produce an insonation pattern of roughly 180 degrees, and were operated in a similar frequency range to the transurethral devices, of 7 to 8 MHz. The technical details of these studies are described in much more detail elsewhere[39,40,44,45] As noted above, among the critical roles of MR imaging in thermal ablation of the prostate using ultrasonic applicators is the ability to guide precise positioning of the transurethral and interstitial applicators within the prostate prior to the ablative procedure. Rapid MR imaging sequences, including spoiled gradient recalled (SPGR) and rapid T2 weighted sequences such as single-shot fast spin echo (SSFSE) can be used repeatedly to monitor device positioning to assure good placement. Transurethral devices, for example, are positioned within the gland, and secured in place by filling the small retention balloon at the entrance to the urinary bladder (Figure 3). As will be shown below, directional interstitial devices may be inserted in any portion of the prostate gland to achieve directed ablation of any desired tissue region.

## Role #3 for MRI: Monitoring of thermal therapy using magnetic resonance thermal imaging (MRTI)

The most critical role of MRI is in monitoring of prostate and periprostatic heating during the ablative process. The ability of MRI to monitor tissue heating in real-time allows targeting of a selected region of the gland for ablation by heating to ablative temperatures in excess of 50° C. while controlling the ablative process so as to avoid damage to adjacent structures such as the rectum. Although a wide range of MRI parameters have been shown to be temperature sensitive[46-48], it is the proton resonance frequency (PRF) temperature dependence which provides the most robust and practical approach to real time magnetic resonance thermal imaging (MRTI). The basic principle allowing the creation of PRF thermal images is the fact that the phase change $\varphi$, detected using gradient recalled images, can be used to create images that directly depict temperature in prostate tissues. It can be

shown that the relationship between the temperature change in tissues ΔT can be expressed as:

$$\Delta T = \frac{\phi - \phi_0}{\gamma \alpha B T E}$$

where $\alpha$ is the temperature change coefficient -.01 ppm/°C for aqueous tissues, $\gamma$ is the gyroagnetic ratio for water protons, B is the main magnetic field strength, TE is the echo time, and $\varphi_0$ is the initial phase before heating begins. Since body temperature is known, the above equation can be used to create phase-sensitive gradient echo images that directly encode local tissue temperature. Such images can be rapidly acquired and displayed at real time rates as overlays on images displaying anatomic detail. Baseline images needed for phase reference were acquired before heating, and MR thermal imaging (MRTI) continued throughout the application of ultrasound energy and during tissue cooling. To correct for baseline drift, the apparent temperature rise in a region of interest (ROI) in adipose tissue adjacent to the prostate was measured, and the values in fat subtracted from data from the entire image. Adding the animal's core temperature to all pixels in the temperature map, the temperature throughout the prostate was displayed in MRTI encoding the temperature range of interest in the range of 47°C to 60°C in a color display. The details of the MRTI computation and display are discussed in much more detail elsewhere[47,49,50]. An example of the utility of MRTI overlays in ablation of prostatic tissue is illustrated in the in vivo study of canine prostate ablation using an interstitial ultrasound applicator are illustrated in Figure 4 below. In Figure 4, images are shown of the ablation of a targeted region of the posterior prostate within a canine obtained using an interstitial applicator inserted using a ventral approach. It can be seen that the real time MRTI (Figure 4A) provides color depiction of the heated region within the prostate gland, and that the tissue ultimately shown to have undergone complete ablation experienced maximal temperatures of at least 52°C., as documented in the tetrazolium choride (TTC) vital stained histologic section at this level (Figure 4C). Such real time depiction of temperature distribution within the prostate with MRTI provides a crucial tool for assuring complete lesion ablation without significant damage to sensitive structures adjacent to the gland (Figure 5), as will be discussed further below.

## Role #4 for MRI: Depiction of ablation within and adjacent to the prostate post-procedure

Following a focal ablation procedure, it is valuable to document complete lesion ablation with preservation of adjacent tissues. Such imaging can be used to direct further ablative efforts if incomplete ablation is initially documented. It has been shown that the distribution of thermally ablated tissues within the prostate can be depicted accurately using contrast enhanced MRI, since the ablated regions are immediately devascularized[51]. As an example of this phenomenon, in the study of the canine prostate shown in Figure 4, thirty days after the ablative procedure, the animal was rescanned prior to sacrifice (Figure 4B), showing a large nonenhancing cavity filled with fluid at the left posterior aspect of the gland in a contrast enhanced image. The TTC stained section of the prostate confirmed complete

resorption of prostate in this circumscribed region (Figure 4C), with creation of a fluid-filled cavity. In all cases in which animals were kept alive for 30 days after ablation complete resorption of ablated prostatic tissue has been noted. Prior in vivo work by Kincaide[52] and Gelet[53] has supported the concept that chronic thermal lesions in prostatic tissue are resorbed, leaving cystic spaces.

## Discussion

In spite of the importance of prostate cancer as the most common nondermatologic malignancy in males, and its status as the second leading cause of male cancer death, the most effective means of treatment remains a perplexing issue. The effectiveness of standard treatments for prostate cancer, particularly for radical prostatectomy (RP) has been called into question by the few randomized prospective trials of RP versus observation. In the large Scandinavian Prostate Cancer Group study[54], metastatic cancer incidence and prostate cancer death, but not overall mortality were reduced in the radical prostatectomy (RP) group at a median of 10.8 years after diagnosis. In the more recently reported PIVOT trial in the USA[55], there was no statistically significant improvement in all-cause or prostate-cancer mortality of localized prostate cancer detected by PSA testing for RP compared to observation, through at least 12 years of follow-up. The RP group was shown, however to have experienced significantly more side effects of incontinence and impotence over the study period. Such recent results have lead to increased interest in minimally invasive techniques for focal prostate cancer ablation, since these offer the possibility of effective treatment with minimal side effects. This review has addressed the important ways in which MRI can assist effective focal ablation of confined prostate cancer. MRI guided focal ablation of the prostate in the manner described, using precisely-directed ultrasonic applicators, or other thermal modalities, appears to have the potential for focal ablation of cancer within the prostate with minimal side effects. While MRI guided focal ablative techniques, including the use of ultrasonic applicators, show promise for focal therapy of prostate cancer, there are a number of important challenges to the clinical implementation of such a treatment strategy. The first challenge, as discussed above, is the inconsistent and suboptimal accuracy of depiction of prostate cancer index lesions within the gland using contemporary MRI techniques. If focal therapy is to become a reality, accurate delineation of tumor volumes must be achieved, since accurate index lesion targeting is essential. Techniques for prostate MRI are continuing to evolve, and further advances do appear likely to offer the promise for accurate index lesion of prostate cancer in the near future as discussed above, in at least a significant subset of patients.

In addition to tumor localization, major challenges are also presented by the possibility of damage to structures adjacent to the prostate gland, since cancers often extend to the gland periphery, raising the possibility of unacceptable collateral damage to sensitive adjacent tissues. If the promise of focal ablation with minimal side effects is to be achieved, prostatic ablation using thermal techniques must avoid or minimize side effects related to rectal, urethral or neurovascular bundle (NVB) damage to the largest extent possible. Some of these problems can be illustrated with reference to Figure 5, an axial T2W MRI through the midportion of the prostate of a 57 year old patient with BPH. Anterior and lateral to the prostate there is no substantial likelihood of significant damage causing morbidity, since the

periprostatic venous plexus, which likely acts to dissipate heat, surrounds the gland. In addition to the critical anterior rectal wall, the posterolateral aspects of the prostate gland are in intimate contact with the bilateral NVB. Seventy percent of prostate cancers arise from the posterior peripheral zone (PZ) of the prostate, adjacent to the rectum and bilateral NVB, and a substantial majority of index prostate cancer lesions will be posteriorly located in very close proximity to these very sensitive structures. The benefit of sparing at least one NVB is strongly supported by the hemiablation studies of prostate cancer by Onik et al.[10] since a far lower incidence of impotence was observed than for radical prostatectomy patients.

The necessity of avoiding rectal damage and potentially creating rectoprostatic fistulae is made clear by experience such as the clinical ablation of prostate cancer by transrectal HIFU[5], whereas in early studies, an incidence of up to 6% of this very serious complication was observed, although subsequent equipment and procedure modification have dramatically reduced this complication rate[1]. A number of possible approaches to mitigating the danger include accurate MRTI to ablate the posterior prostate while avoiding the rectum, endorectal cooling devices to lower rectal wall temperature during treatment, and the creation of barriers between the prostate and the rectal wall. Rectal cooling systems have been described for minimizing rectal damage and simulations and in vivo work[56,57] have indicated that such an approach has value, but it is not difficult to imagine the rectal cooling being overtaken by transmitted heating from the prostate. Yet another innovative approach to rectal preservation is that of Lancaster and Toi[58], who have described a “hydrodissection” technique for isolating the rectum from the prostate during microwave hyperthermia, creating an effective thermal barrier. Of the two types of ultrasonic applicators discussed, the interstitial applicators may have advantages for ablation of prostate cancer with preservation of sensitive normal posterior structures. These applicators can be directional to, for example, a 180 degree sector, and may be inserted posteriorly and peripherally within the gland with ultrasonic energy directed anteriorly, away from the rectum and NVB's.

Damage to the prostatic urethra can also be a serious problem, as can be inferred from transrectal HIFU studies of prostate cancer, since up to 7% of patients undergoing this procedure have experienced incontinence. Additionally, urinary retention in patients in patients undergoing transrectal HIFU for cancer treatment is such a common problem that the procedure is generally accompanied by surgical TURP[5] at present. Damage to the prostatic urethra can be prevented in ablations using transurethral devices, since the intraprostatic cooling balloon cools and protects the prostatic urethra as well as the piezoelectric emitters. In addition to the in vivo canine studies presented above, in recent years there has been application of transurethral applicators, to initial human studies[59,60]. Rotational control of applicators was performed, and using MRTI it was shown in prostatectomy patients that controlled ablation in vivo in patients is indeed possible, giving encouragement for eventual clinical utility.

Although the challenges discussed above must be acknowledged and ultimately addressed, MRI guidance provides a wealth of useful imaging information capable of greatly assisting the ablation process. The roles for MRI in aiding precise device location, providing accurate thermal monitoring of the ablative process and depiction of tissue ablation post-procedure are all achievable with remarkable accuracy, as demonstrated in this review and supported

by the literature. MRI compatible transurethral and interstitial ultrasound applicators have been shown capable of accurate and complete ablation of targeted prostate tissue in vivo, and appear highly suitable as one technique among many promising thermal approaches for focal ablation of confined prostate cancer. Exploitation of the four roles suggested for MRI guidance of the ablative procedure seems a practical and promising approach to focal thermal therapy of prostate cancer.

## Acknowledgments

The MR images shown in Figure 1 were obtained under the direction of Sharon Clarke MD of the Department of Radiology, and the pathologic mapping in this Figure was performed by Jesse McKenney of the Department of Urology, both of the Stanford University School of Medicine. The clinical study of prostate MRI has been supported by General Electric Corporation. The work described in this paper was supported by grants R01 CA11198, R01 CA122276, R21 CA137472, P01 CA159992, and R01 CA121163 from the NIH.

## References

1. Crouzet S, Rebillard X, Chevallier D, et al. Multicentric oncologic outcomes of high-intensity focused ultrasound for localized prostate cancer in 803 patients. Eur. Urol. 2010; 58(4):559–566. [PubMed: 20619958]
2. Lian H, Guo H, Gan W, et al. Cryosurgery as primary treatment for localized prostate cancer. Int Urol Nephrol. 2011; 43(4):1089–1094. [PubMed: 21475948]
3. Bouza C, López T, Magro A, et al. Systematic review and meta-analysis of Transurethral Needle Ablation in symptomatic Benign Prostatic Hyperplasia. BMC Urol. 2006; 6:14. [PubMed: 16790044]
4. Colin P, Mordon S, Nevoux P, et al. Focal laser ablation of prostate cancer: definition, needs, and future. Adv Urol. 2012; 2012:589160. [PubMed: 22666240]
5. Rouvière O, Souchon R, Salomir R, et al. Transrectal high-intensity focused ultrasound ablation of prostate cancer: effective treatment requiring accurate imaging. Eur J Radiol. 2007; 63(3):317–327. [PubMed: 17689218]
6. Aus G. Current Status of HIFU and Cryotherapy in Prostate Cancer – A Review. European Urology. 2006; 50(5):927–934. [PubMed: 16971038]
7. Mouraviev V, Polascik TJ. Update on cryotherapy for prostate cancer in 2006. Current opinion in urology. 2006
8. Bahn D, de Castro Abreu AL, Gill IS, et al. Focal cryotherapy for clinically unilateral, low-intermediate risk prostate cancer in 73 men with a median follow-up of 3.7 years. Eur. Urol. 2012; 62(1):55–63. [PubMed: 22445223]
9. Algaba F, Montironi R. Impact of prostate cancer multifocality on its biology and treatment. J. Endourol. 2010; 24(5):799–804. [PubMed: 20367408]
10. Onik G, Vaughan D, Lotenfoe R, et al. The “male lumpectomy”: focal therapy for prostate cancer using cryoablation results in 48 patients with at least 2-year follow-up. Urol. Oncol. 2008; 26(5): 500–505. [PubMed: 18774463]
11. Noguchi M, Stamey TA, McNeal JE, et al. Prognostic factors for multifocal prostate cancer in radical prostatectomy specimens: lack of significance of secondary cancers. J. Urol. 2003; 170(2 Pt 1):459–463. [PubMed: 12853799]
12. Wise AM, Stamey TA, McNeal JE, et al. Morphologic and clinical significance of multifocal prostate cancers in radical prostatectomy specimens. Urology. 2002; 60(2):264–269. [PubMed: 12137824]
13. Gangi A, Tsoumakidou G, Abdelli O, et al. Percutaneous MR-guided cryoablation of prostate cancer: initial experience. Eur Radiol. 2012; 22(8):1829–1835. [PubMed: 22752525]
14. Lecornet E, Ahmed HU, Moore CM, et al. Conceptual basis for focal therapy in prostate cancer. J. Endourol. 2010; 24(5):811–818. [PubMed: 20443699]

15. Lecornet E, Ahmed HU, Moore C, et al. Focal therapy for prostate cancer: a potential strategy to address the problem of overtreatment. Arch. Esp. Urol. 2010; 63(10):845–852. [PubMed: 21187566]
16. Jones JS. Focal or subtotal therapy for early stage prostate cancer. Curr Treat Options Oncol. 2007; 8(3):165–172. [PubMed: 17701110]
17. Villers A, McNeal JE, Freiha FS, et al. Multiple cancers in the prostate. Morphologic features of clinically recognized versus incidental tumors. Cancer. 1992; 70(9):2313–2318. [PubMed: 1382830]
18. Freiha FS, McNeal JE, Stamey TA. Selection criteria for radical prostatectomy based on morphometric studies in prostate carcinoma. NCI Monogr. 1988; (7):107–108. [PubMed: 3173495]
19. Liu W, Laitinen S, Khan S, et al. Copy number analysis indicates monoclonal origin of lethal metastatic prostate cancer. Nat. Med. 2009; 15(5):559–565. [PubMed: 19363497]
20. Ahmed HU. The index lesion and the origin of prostate cancer. N. Engl. J. Med. 2009; 361(17): 1704–1706. [PubMed: 19846858]
21. Onik G, Barzell W. Transperineal 3D mapping biopsy of the prostate: an essential tool in selecting patients for focal prostate cancer therapy. Urol. Oncol. 2008; 26(5):506–510. [PubMed: 18774464]
22. Langer DL, van der Kwast TH, Evans AJ, et al. Prostate cancer detection with multi-parametric MRI: logistic regression analysis of quantitative T2, diffusion-weighted imaging, and dynamic contrast-enhanced MRI. J Magn Reson Imaging. 2009; 30(2):327–334. [PubMed: 19629981]
23. Weinreb JC, Blume JD, Coakley FV, et al. Prostate cancer: sextant localization at MR imaging and MR spectroscopic imaging before prostatectomy--results of ACRIN prospective multi-institutional clinicopathologic study. Radiology. 2009; 251(1):122–133. [PubMed: 19332850]
24. Quint LE, Van EJ, Bland PH, et al. Prostate cancer: correlation of MR images with tissue optical density at pathologic examination. Radiology. 1991; 179(3):837–842. [PubMed: 2028002]
25. Sommer FG, Nghiem HV, Herfkens R, et al. Determining the volume of prostatic carcinoma: value of MR imaging with an external-array coil. AJR Am J Roentgenol. 1993; 161(1):81–86. [PubMed: 8517328]
26. Saritas EU, Cunningham CH, Lee JH, et al. DWI of the spinal cord with reduced FOV single-shot EPI. Magn Reson Med. 2008; 60(2):468–473. [PubMed: 18666126]
27. Saranathan M, Rettmann DW, Hargreaves BA, et al. DIfferential subsampling with cartesian ordering (DISCO): A high spatio-temporal resolution dixon imaging sequence for multiphasic contrast enhanced abdominal imaging. J Magn Reson Imaging. 2012
28. Katahira K, Takahara T, Kwee TC, et al. Ultra-high-b-value diffusion-weighted MR imaging for the detection of prostate cancer: evaluation in 201 cases with histopathological correlation. Eur Radiol. 2011; 21(1):188–196. [PubMed: 20640899]
29. Kim CK, Park BK, Kim B. High-b-value diffusion-weighted imaging at 3 T to detect prostate cancer: comparisons between b values of 1,000 and 2,000 s/mm2. AJR Am J Roentgenol. 2010; 194(1):W33–7. [PubMed: 20028888]
30. Turkbey B, Xu S, Kruecker J, et al. Documenting the location of systematic transrectal ultrasound-guided prostate biopsies: correlation with multi-parametric MRI. Cancer Imaging. 2011; 11:31–36. [PubMed: 21450548]
31. Fütterer JJ, Barentsz JO. MRI-guided and robotic-assisted prostate biopsy. Curr Opin Urol. 2012; 22(4):316–319. [PubMed: 22617059]
32. Turkbey B, Mani H, Shah V, et al. Multiparametric 3T prostate magnetic resonance imaging to detect cancer: histopathological correlation using prostatectomy specimens processed in customized magnetic resonance imaging based molds. J. Urol. 2011; 186(5):1818–1824. [PubMed: 21944089]
33. Delongchamps NB, Rouanne M, Flam T, et al. Multiparametric magnetic resonance imaging for the detection and localization of prostate cancer: combination of T2-weighted, dynamic contrast-enhanced and diffusion-weighted imaging. BJU Int. 2011; 107(9):1411–1418. [PubMed: 21044250]

34. Bittencourt LK, Barentsz JO, de Miranda LCD, et al. Prostate MRI: diffusion-weighted imaging at 1.5T correlates better with prostatectomy Gleason Grades than TRUS-guided biopsies in peripheral zone tumours. Eur Radiol. 2012; 22(2):468–475. [PubMed: 21913058]
35. Nau WH, Diederich CJ, Burdette EC. Evaluation of multielement catheter-cooled interstitial ultrasound applicators for high-temperature thermal therapy. Med Phys. 2001; 28(7):1525–1534. [PubMed: 11488586]
36. Diederich CJ, Stafford RJ, Nau WH, et al. Transurethral ultrasound applicators with directional heating patterns for prostate thermal therapy: in vivo evaluation using magnetic resonance thermometry. Med Phys. 2004; 31(2):405–413. [PubMed: 15000627]
37. Diederich CJ, Nau WH, Stauffer PR. Ultrasound applicators for interstitial thermal coagulation. IEEE Trans. Ultrason. Ferroelectr. Freq. Control (USA). 1999; 46(5):1218–1228.
38. Ross AB, Diederich CJ, Nau WH, et al. Curvilinear transurethral ultrasound applicator for selective prostate thermal therapy. Med Phys. 2005; 32(6):1555–1565. [PubMed: 16013714]
39. Ross AB, Diederich CJ, Sommer G, et al. Highly directional transurethral ultrasound applicators with rotational control for MRI-guided prostatic thermal therapy. Phys Med Biol. 2004; 49(2): 189–204. [PubMed: 15083666]
40. Nau WH, Diederich CJ, Ross AB, et al. MRI-guided interstitial ultrasound thermal therapy of the prostate: a feasibility study in the canine model. Med Phys. 2005; 32(3):733–743. [PubMed: 15839345]
41. Diederich CJ, Nau WH, Burdette EC, et al. Combination of transurethral and interstitial ultrasound applicators for high-temperature prostate thermal therapy. Int J Hyperthermia. 2000; 16(5):385–403. [PubMed: 11001573]
42. Ross AB, Diederich CJ, Nau WH, et al. Highly Directional Transurethral Ultrasound Applicators with Rotational Control for MRI Guided Prostatic Thermal Therapy. Phys Med Biol. 2004; 49(1): 189–204. [PubMed: 15083666]
43. Diederich CJ. Interstitial ultrasound applicators are practical from an engineering perspective for treating large tumours [letter; comment]. Int J Hyperthermia. 1996; 12(2):305–306. [PubMed: 8926398]
44. Kinsey AM, Diederich CJ, Tyreus PD, et al. Multisectored interstitial ultrasound applicators for dynamic angular control of thermal therapy. Med Phys. 2006; 33(5):1352–1363. [PubMed: 16752571]
45. Kinsey AM, Diederich CJ, Rieke V, et al. Transurethral ultrasound applicators with dynamic multi-sector control for prostate thermal therapy: in vivo evaluation under MR guidance. Med Phys. 2008; 35(5):2081–2093. [PubMed: 18561684]
46. Chen J, Daniel BL, Diederich CJ, et al. Monitoring prostate thermal therapy with diffusion-weighted MRI. Magn Reson Med. 2008; 59(6):1365–1372. [PubMed: 18506801]
47. Rieke V, Kinsey AM, Ross AB, et al. Referenceless MR thermometry for monitoring thermal ablation in the prostate. IEEE Trans Med Imaging. 2007; 26(6):813–821. [PubMed: 17679332]
48. Rieke V, Vigen KK, Sommer G, et al. Referenceless PRF shift thermometry. Magn Reson Med. 2004; 51(6):1223–1231. [PubMed: 15170843]
49. Pauly KB, Diederich CJ, Rieke V, et al. Magnetic resonance-guided high-intensity ultrasound ablation of the prostate. Top Magn Reson Imaging. 2006; 17(3):195–207. [PubMed: 17414077]
50. Holbrook A, Santos J, Kaye E. Real-time MR thermometry for monitoring HIFU ablations of the liver - Holbrook - 2009 - Magnetic Resonance in Medicine - Wiley Online Library. Magnetic .... 2010
51. Boyes A, Tang K, Yaffe M, et al. Prostate tissue analysis immediately following magnetic resonance imaging guided transurethral ultrasound thermal therapy. J. Urol. 2007; 178(3 Pt 1): 1080–1085. [PubMed: 17644137]
52. Kincaide LF, Sanghvi NT, Cummings O, et al. Noninvasive ultrasonic subtotal ablation of the prostate in dogs. Am. J. Vet. Res. 1996; 57(8):1225–1227. [PubMed: 8836379]
53. Gelet A, Chapelon JY, Margonari J, et al. Prostatic tissue destruction by high-intensity focused ultrasound: experimentation on canine prostate. J. Endourol. 1993; 7(3):249–253. [PubMed: 8358423]

54. Bill-Axelson A, Holmberg L, Filén F. Radical Prostatectomy Versus Watchful Waiting in Localized Prostate Cancer: the Scandinavian Prostate Cancer Group-4 Randomized Trial. National Cancer . 2008

55. Wilt TJ, Brawer MK, Jones KM, et al. Radical prostatectomy versus observation for localized prostate cancer. N. Engl. J. Med. 2012; 367(3):203–213. [PubMed: 22808955]

56. Nau, N.; Diederich, C.; Ross, A., et al. Evaluation of Endorectal and Urethral Cooling Devices during MR-Guided Ultrasound Thermal Ablation in Canine Prostate. IEEE; San Francisco, CA, USA: Sep 1-5. 2004 p. 2492-2495.2004

57. Burtnyk M, Chopra R, Bronskill M. Simulation study on the heating of the surrounding anatomy during transurethral ultrasound prostate therapy: A 3D theoretical analysis of patient safety. Med Phys. 2010; 37(6):2862. [PubMed: 20632598]

58. Lancaster C, Toi A, Trachtenberg J. Interstitial microwave thermoablation for localized prostate cancer. Urology. 1999; 53(4):828–831. [PubMed: 10197869]

59. Da Rosa MR, Trachtenberg J, Chopra R, et al. Early experience in MRI-guided therapies of prostate cancer: HIFU, laser and photodynamic treatment. Cancer Imaging. 2011:11. Spec No A:S3–8.

60. Siddiqui K, Chopra R, Vedula S, et al. MRI-guided transurethral ultrasound therapy of the prostate gland using real-time thermal mapping: initial studies. Urology. 2010; 76(6):1506–1511. [PubMed: 20709381]

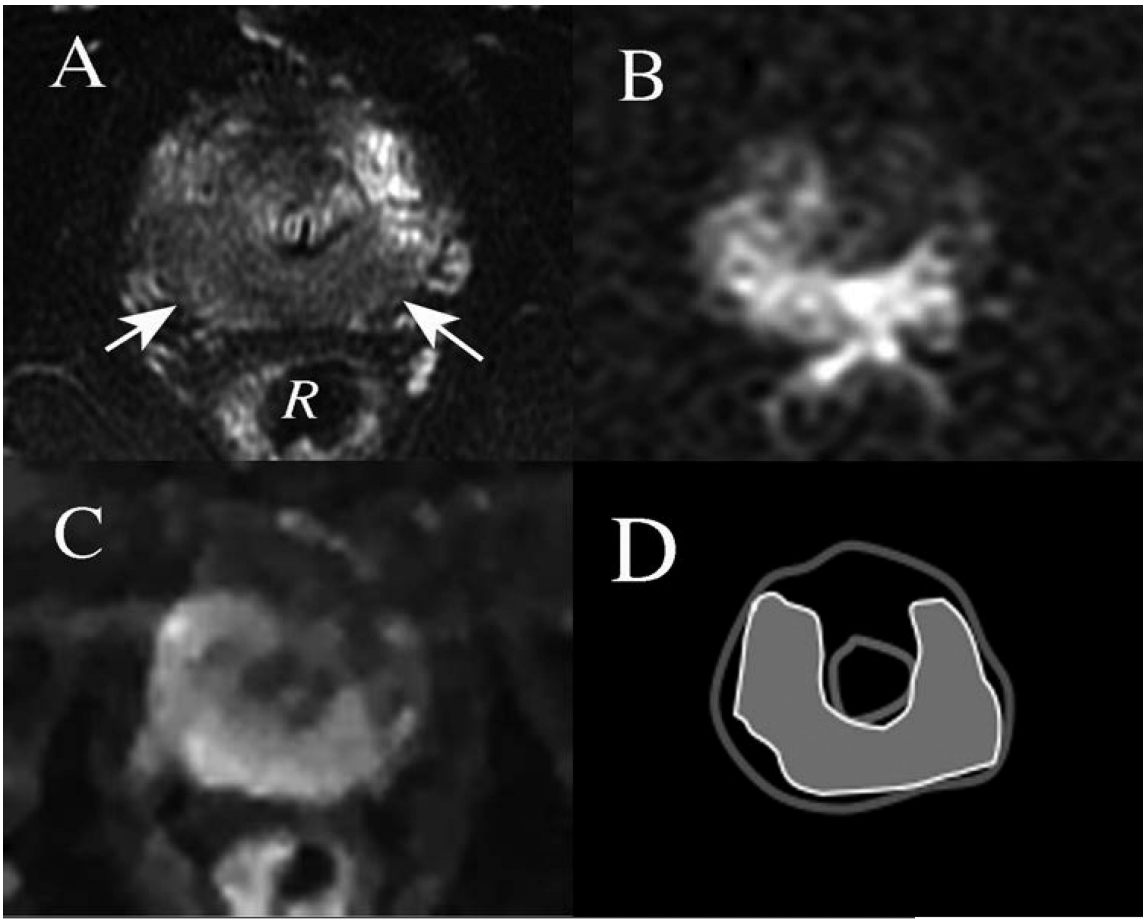


**Figure 1.**

Axial images at level of the prostatic apex obtained in a 3 Tesla scanner, of a patient with biopsy-proved prostate cancer prior to radical prostatectomy. A) T2-weighted image shows large region of decreased signal intensity posteriorly (arrows). *R* = Rectum. B) Reduced field of view Diffusion weighted image (Rfov DWI) obtained using high b value (b=1600 s/mm$^2$) shows high signal intensity roughly corresponding to the low signal region in the T2-weighted image C) Dynamic contrast enhanced (DCE) image displaying maximal enhancement in early arterial phase also indicates early enhancement of a similar region in the apex of the prostate gland. D) Pathologic map showing the distribution of cancer in gray, found in prostatectomy specimen at this level in the gland.

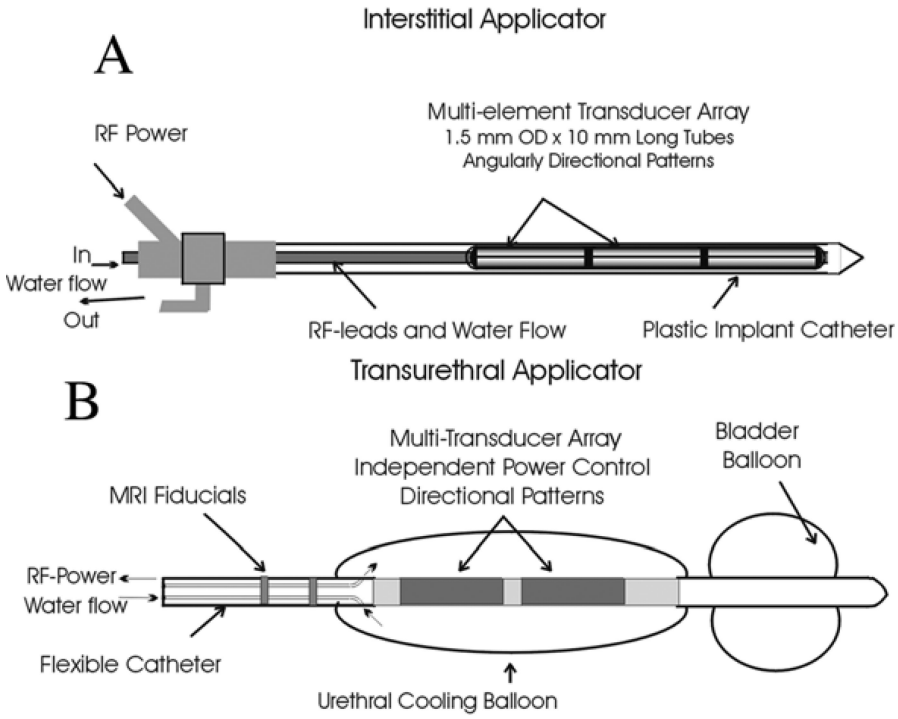


**Figure 2.**

Diagrammatic representation of A) Interstitial and B) Transurethral ultrasonic applicators designed for targeted ablation of prostate tissue under MRI guidance. Interstitial applicators, designed for direct insertion into the prostate through the perineum, consist of several independently driven cylindrical piezoelectric elements that may be etched to create emitted ultrasonic patterns in desired angular patterns. Transurethral applicators incorporate urethral cooling balloons that also cool the piezoelectric elements, and which may be planar, curvilinear or cylindrical in shape. The bladder balloon is used to retain the device in position within the prostatic urethra. Both types of applicators are constructed using non-ferromagnetic materials which might create artifacts in MR images.

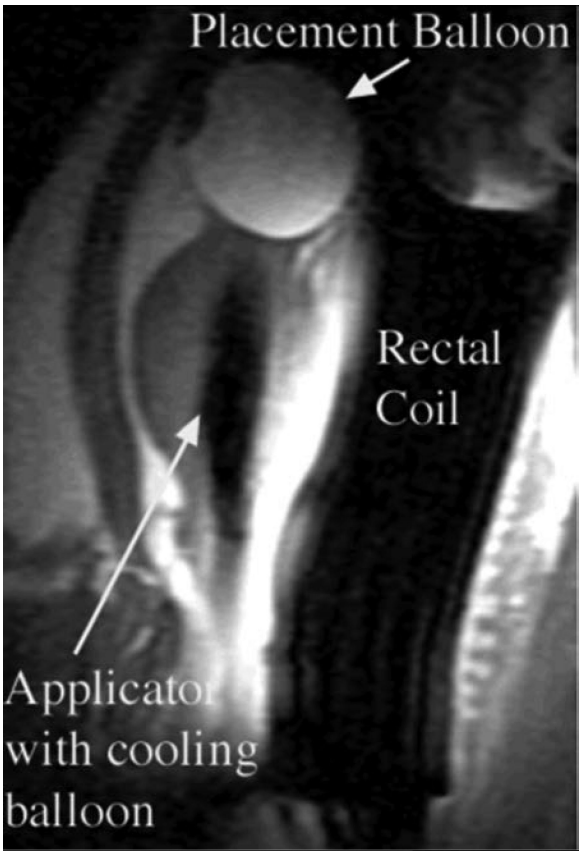


**Figure 3.**

Sagittal SPGR T1-weighted image from study of ablation of a canine prostate using a transurethral applicator incorporating a cooling balloon within the prostate. The device uses circulating water to cool both transducers and the prostatic urethra. A placement balloon in the urinary bladder, containing dilute gadolinium contrast to enhance visualization, retains the applicator in position. The rectal coil arrangement both enhances SNR for prostatic imaging, and incorporates circulating water for rectal cooling.

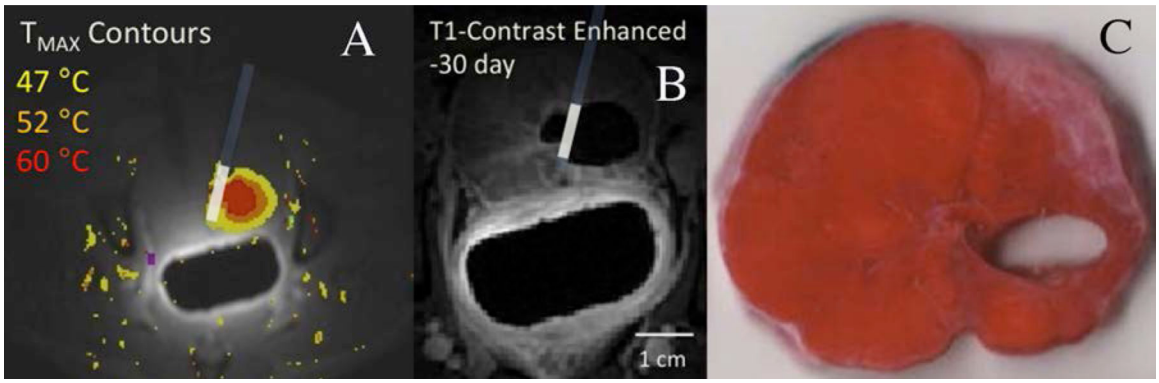


**Figure 4.**

Study of the use of directional interstitial probe in ablation of a posterior region of canine prostate in vivo. In A) and B), the location of the interstitial probe, with ultrasound energy directed away from the urethra, is indicated. A) Axial MRTI through ablation region in prostate, with color overlay indicating temperatures from 47°C to 60°C, leading to ablation over 15 minutes. B) contrast-enhanced MRI at the same level in the prostate obtained 30 days later, showing dark region adjacent to the applicator, corresponding to the zone of tissue ablated. C) Corresponding TTC-stained pathologic section of prostate harvested 30 days post ablation shows tissue defect resulting from apparent resorption of prostate tissue in the zone of ablation.

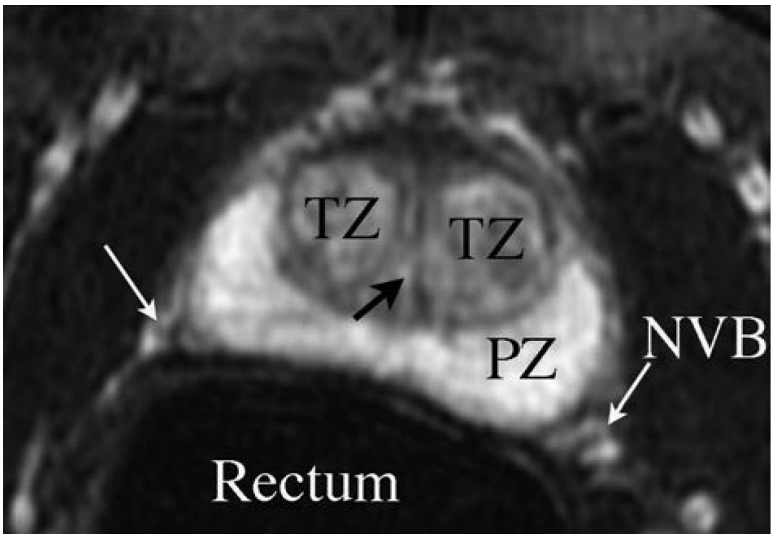


**Figure 5.**

T2 weighted axial MRI through midportion of a prostate of a patient with moderate BPH. Enlarged transition zone (TZ) lobes are seen anterolateral to the prostatic urethra (black arrow), and there is clear differentiation of the TZ from the more posterior peripheral zone (PZ). Adjacent critical structures which are at risk for damage during ablation include the bilateral neurovascular bundles (NVB) indicated with white arrows, and the rectum.